Title	Smart imaging using laser targeting: a multiple barcodes application
Authors	Amin, M. Junaid;Riza, Nabeel A.
Publication date	2014-05-15
Original Citation	Amin, M. J. and Riza, N. A. (2014) "Smart imaging using laser targeting: a multiple barcodes application", Proceedings of SPIE, 9141, Optical Sensing and Detection III, 91411H (15 May), SPIE Photonics Europe, 2014, Brussels, Belgium. doi: 10.1117/12.2047596
Type of publication	Conference item
Link to publisher's version	10.1117/12.2047596
Rights	© 2014 Society of Photo-Optical Instrumentation Engineers (SPIE). One print or electronic copy may be made for personal use only. Systematic reproduction and distribution, duplication of any material in this paper for a fee or for commercial purposes, or modification of the content of the paper are prohibited.
Download date	2024-04-19 00:15:16
Item downloaded from	https://hdl.handle.net/10468/10067

PROCEEDINGS OF SPIE

Smart imaging using laser targeting: a multiple barcodes application

Amin, M. Junaid, Riza, Nabeel

SPIE.

Smart Imaging Using Laser Targeting:
A Multiple Barcodes Application

M. Junaid Amin and Nabeel A. Riza[a,b*]

[a,b]Electrical and Electronic Engineering, School of Engineering, University College Cork (UCC), College Road, Cork, Ireland

*email: n.riza@ucc.ie

ABSTRACT

To the best of our knowledge, proposed is a novel variable depth of field smart imager design using intelligent laser targeting for high productivity multiple barcodes reading applications. System smartness comes via the use of an Electronically Controlled Variable Focal-Length Lens (ECVFL) to provide an agile pixel (and/or pixel set) within the laser transmitter and optical imaging receiver. The ECVFL in the receiver gives a flexible depth of field that allows clear image capture over a range of barcode locations. Imaging of a 660 nm wavelength laser line illuminated 95-bit one dimensional barcode is experimentally demonstrated via the smart imager for barcode target distances ranging from 10 cm to 54 cm. The smart system captured barcode images are evaluated using a proposed barcode reading algorithm. Experimental results after computer-based post-processing show a nine-fold increase in barcode target distance variation range (i.e., range variation increased from 2.5 cm to 24.5 cm) when compared to a conventional fixed lens imager. Applications for the smart imager include industrial multiple product tracking, marking, and inspection systems.

Keywords: Optical Sensing, Industrial inspection, imaging systems, pattern recognition, and target tracking

1. INTRODUCTION

Optical imaging systems play a vital role in a variety of applications including industrial inspection, patient monitoring and security surveillance [1-4]. These imagers capture visual representations of objects in the form of images which are then analysed via human intervention or software processing. To obtain desirable clear snapshots for effective post-processing, objects of interest need to be located within the depth of field of an imaging system. For conventional imagers comprising fixed focal length imaging lenses, the depth of field is constant. Various barcode imaging techniques have been proposed in literature [5-9] and in general, these barcode imagers have a restricted barcode positional range due to their fixed depth of field. In addition, prior-art barcode scanners do not provide target specific intelligence to the laser targeting mechanism via programmable beamforming that can add additional capabilities to the overall transmit-receive active (i.e., laser illuminated) imager using the agile pixel (and/or pixel set) concept.

One application where conventional imagers are used is industrial tracking via product tagged barcodes. As shown in Fig. 1(a), a conventional optical Transmitter/ Receiver (T/R) identifies products via their barcode images as the items move on a single industrial conveyer belt. The depth of field of a conventional T/R is indicated by the barcode readable scan angle which is limited to within the dashed lines shown in Fig. 1(a). If multiple conveyer belts are run in parallel to increase industrial productivity, the conventional T/R cannot track barcodes along the multiple parallel tracks as these conveyer belts lie outside the depth of field of the conventional T/R. This is because the distance of the T/R from each of the tracks is different for different conveyer belts.

Thus, proposed in this paper is the use of a smart T/R for optical targeting and reception that has a variable depth of field to accommodate for the varying distances so as to ensure clear snapshots of the items (e.g., barcodes) on the different conveyer belts. Prior efforts to vary the depth of field in imaging systems has involved the use of mechanical motion of lenses, although at the expense of wear and tear due to moving parts, slow target object detection time, and increase in overall system size. Thus, a smart active (i.e., laser-based) imaging system is desired that can increase the target readable range while achieving a compact size and a fast operations time along with target feature-based laser beam conditioning. The use of the smart T/R as shown in Fig. 1(b) allows high quality imaging operation for different path lengths L_1, L_2 …L_N (see Fig.1(c)) when using multiple conveyor belts.

2. PROPOSED SMART TRANSMITTER/RECEIVER FOR MULTIPLE BARCODE APPLICATION

Previously, the use of an Electronically Controlled Variable Focal Focal-Length Lens (ECVFL) has been proposed and demonstrated for both transmit and receive agile optical systems [10-14]. With the same motivation, Fig. 2(a) shows the proposed smart T/R using ECVFLs for laser targeted imaging of barcodes. The smart transmitter (T) contains an optimized laser source such as a laser line source combined with an ECVFL (not shown in Fig.2(a)) and other beamforming optics (e.g., diffractive optical elements) where these optics produce the desired laser beam contour at the target location that maximizes target optical response. A classic contour is a laser line commonly used for reading optical barcodes. The smart receiver (R) in the T/R also uses an ECVFL along with a bias lens BL (see Fig.2(b)) to provide clear in-focus images of the mirror scanned barcodes at varying distances from the module location. The smart transmitter design would be similar to the smart receiver design, except the detector is replaced by the laser. One can even use the same optics for both the receiver and transmitter if the T and R channels are separated using an optic like a classic beam splitter or custom polarization control optics (e.g., Faraday rotator). The proposed active T/R imager's depth of field is varied by electronically changing the focal length of the ECVFL in the R to account for different barcode locations such as distances L_1, L_2 …L_N shown in Fig.1(c). In Fig.2(b), light scattered off the barcode travels a distance d_2 to pass through the ECVFL-BL arrangement in R to reach the detector array. The ECVFL in R has a variable focal length F_e, and BL is of fixed focal length F_b. Both these lenses are separated by a distance d_1, while the BL and detector array are separated by d_0. Introduction of the bias lens BL serves to increase the T/R imager's field of view and forms the barcode image nearer to the ECVFL in R, reducing the overall T/R imager design size. For a clear image to fall on the detector array, the imaging condition for the 2-lens system must be satisfied for a certain location of the barcode [15]. Change in barcode-detector distance results in barcode image formation outside the plane of the detector array. This barcode position variation can cause image blurring, rendering the barcode difficult to read even using computer post-processing.

Fig. 3 consists of the ray-trace diagrams for the 2-lens system in the R which illustrates the effect of the change in object location on image location, and how the proposed design caters for that change. d_0, d_1 and F_b are kept constant. In Fig. 3(a), with $d_2=d_{21}$ and $F_e=F_{e1}$, application of the ray-trace procedure [15] shows that the resulting image falls on the detector plane. When the object is brought closer to the ECVFL in R so that $d_2=d_{22}$ where $d_{22} < d_{21}$ (see Fig. 3(b)), the image is formed out of the detector array's plane, resulting in blurred image formation on the detector itself. This detrimental effect, which is common to prior-art barcode readers encountering objects over a wide range of locations, is overcome in the smart T/R via changing F_e to $F_e = F_{e2}$ where $F_{e2} < F_{e1}$. The change in the ECVFL focal length in R causes the image to form clearly onto the plane of the detector array as shown by the ray-trace diagram in Fig. 3(c). Therefore the change in location of the object or barcode is accommodated by the smart imaging system resulting in clear image formation on the detector array.

3. BARCODE IMAGING EXPERIMENT

To conduct a first stage proof of concept experiment, a laser line source without the ECVFL and extra beamforming optics is used to form the smart T that is deployed for illuminating a Universal Product Code (UPC) 95 bit, 2.5 cm wide one dimensional barcode. Specifically, a Prophotonix's 3D Pro 3.3 mW 660 nm wavelength laser line source is used which has a minimum laser line spatial width of 90 μm at 18.5 cm from the exit point of the T laser module and has a fan angle of 20 degrees. Note that future work will engage an ECVFL in the T to adjust the laser targeting beam for optimal target location and feature-based optical response. For the present paper, the one dimensional barcode used in the experiment is well illuminated by a laser line and hence the ECVFL in the T is not engaged. The ECVFL used in the R for the experiment is the Optotune EL-10-30 VIS LD, an electromagnetically actuated mechanical membrane deforming liquid based lens which has a focal length range from 4.5 cm to 12 cm. The fixed focal length F_b of BL is 5 cm, and a Sony CCD imager XC-77 is used as the detector array. The entrance of the imager, i.e., the centre of the ECVFL in the R, is located 6 cm from the exit point of the T laser module. d_0 is chosen to be 1.9 cm, and d_1 is kept to 4.2 cm. For the experiment, the barcode distance d_2 is varied from 10 cm to 54 cm. First, for smart imaging, the ECVFL focal length F_e in R is adjusted for each barcode location to ensure the detector array captures focussed barcode images. Then, to compare the smart T/R performance to a fixed lens imaging system, F_e is fixed to 4.7 cm giving in-focus images for $d_2 = 14.2$ cm and F_e is left unchanged for all other values of d_2. This fixed setting of F_e constitutes a conventional fixed lens

imager. Images captured using both smart and conventional fixed lens methods are displayed in Fig. 4 for d_2 values of 14.2 cm, 17.5 cm and 34.5 cm. In Fig. 4(a), images acquired via both methods are the same since both imagers are focused onto the barcode placed at $d_2 = 14.2$ cm. However, for $d_2 = 17.5$ cm (Fig. 4(b)), the image plane for the fixed lens system is different from the detector plane, giving a blurred image on the CCD. The smart T/R accommodates for the shift in object (barcode) location and keeps the image plane on the CCD, as explained in Fig. 3, giving a clear and readable image (Fig. 4(b)). The image clarity for the fixed lens imager is further deteriorated at $d_2 = 34.5$ cm while the smart active imager keeps the laser illuminated barcode in focus (Fig. 4(c)).

A barcode reading algorithm is used to evaluate barcode readability for both smart and fixed lens methods for the range of barcode locations. Many barcode decoding techniques that are present in the literature include Hough transform, convolution analysis, and waveform analysis [16-19]. Presented here is an algorithm based on peak recognition and thresholding, which is used to analyse the effectiveness of the smart imager. The algorithm implemented in Matlab is described in the following precise steps. Step 1: The raw barcode image of Fig. 5(a) is first converted to grayscale before the intensity values in each column are summed up over all the rows and then normalized, giving a 1-D intensity profile along the horizontal axis of the barcode. Step 2: The useful region of the image, which contains the barcode binary pattern, is extracted by executing a strategic "for" loop to pinpoint the column index where the consecutive intensities above a set threshold terminate. The loop is applied to both beginning and concluding portions of the barcode to ensure correct start and end points of the binary pattern. The result of Step 2 is shown in Fig. 5(b). Step 3: The local maxima and minima of the extracted binary intensity pattern in Step 2 are found, using appropriate thresholds to ensure alternating maxima and minima locations. Then, between consecutive maxima and minima, the midpoint intensity values are found, and those are used as thresholds to approximate the binary code (see Fig. 5(c)). Step 4: Finally, the obtained approximate binary code is down-sampled, and rounded off to 95 bit (UPC standard). The algorithm is applied to Fig. 4 (b) images, taken at $d_2 = 17.5$ cm to compare barcode readability for images captured via the smart T/R imager and fixed lens methods, and the results are given in Fig. 6.

Fig. 6 illustrates superior barcode readability using the smart T/R versus fixed lens imaging systems. The percentage of barcode recovered via the algorithm application on images captured via the smart T/R is 94.7 % at $d_2 = 17.5$ cm. For the same value of d_2, the algorithm recovers 46.8 % barcode from the image captured via the fixed lens mode of the T/R. This result is expected owing to the clear barcode images available for post-processing using the proposed smart imager design. The fixed lens imager gives a 2.5 cm dynamic range with d_2 from 13.5 cm to 16.0 cm, while the proposed smart imager provides a dynamic range with d_2 from 10.0 cm to 34.5 cm, giving a nine-fold increase in imager dynamic range. The dynamic range for both imagers is measured over a d_2 range over which images captured give barcode recovery percentages greater than 65 % via the algorithm application. Note that although barcode readability via the smart T/R is much improved for the range of d_2, compared to a fixed lens imager, the overall image clarity is reduced with increasing distance due to a number of factors. The limited pixel resolution of the deployed detector array restricts the amount of resolvable spatial frequencies of the barcode. Specifically, the deployed CCD has a pixel pitch of 11 μm and has 768 × 493 pixels. Fig. 4 images of the barcode at $d_2 = 34.5$ show barcode lines to be closer together than in images captured at $d_2 = 17.5$ cm. The reduced spatial sampling of the barcode pattern in images taken at larger d_2, along with limited pixel quantity of the detector array, decreases the image quality available for post processing. Aberration effects across the two-lens system further deteriorates image quality with increased target distance. The post processing algorithm used in the experiment also has its limitations. For example, uncertainties arising during the down-sampling in Step 4 increase the error in the barcode bits which may cause a right or left shift in the algorithm read barcode, dramatically decreasing the recovery percentage. Lack of calibrated distance based algorithm conditions result in incorrect thresholds to be set in Step 2, making the data recovery process less precise. Incorrect maxima and minima recognition in Step 3 along with optical noise present in the system introduces further errors. The imager aberration and spatial frequency limit issues can be significantly reduced using commercially available cameras with high pixel density and low aberration optics, and then modifying them to include the ECVFL to allow for the extended barcode readability range. Post processing steps can also be refined via application of more sophisticated algorithms for effective decoding. These improvements will extend the readability range of the smart T/R, making it suitable for industrial deployment.

The operational speed of the smart T/R is determined by a number of factors that includes the scanning speed of the laser scan mirror, the laser power level and sensitivity of the detector array, the contour of the laser illumination on the target, the integration time of the detector array to produce an adequate image for computer-based post-processing, the complexity of the bar-code reading algorithm, the speed of the target/barcode on the conveyor belt, the background light noise level, and environmental (air currents, vibrations, air dust content) conditions of the laser targeting scenario. Today, fast 1 KHz or faster scan mirrors and ECVFL technologies are available including high sensitivity CCD and high speed CMOS cameras. Moreover, the novel use of the ECVFL in the smart transmitter acts as a distance sensor [20], allowing formation of an effective feedback loop between the T and R modules, ensuring the extended DOF of the smart T/R imager. Thus, an optimally engineered smart T/R imager can produce high impact for several industrial imaging applications

4. CONCLUSION

Presented and demonstrated is a smart active imager suited for the industrial barcode reading applications. The demonstrated smart T/R imager uses laser line targeting in combination with an ECVFL that dynamically changes the receive imager's focal length and depth of field allowing clear image capture. A proof of concept experiment is conducted using a low power visible laser line source for barcode targeting of a 95 bit one dimensional barcode. The smart active imager experimental results are compared to those captured using a fixed lens imager. A barcode reading algorithm is proposed to test the barcode readability of the acquired images. Algorithm results show a nine-fold increase in dynamic range of readable barcode T/R to target distances using the proposed smart T/R imager versus the fixed lens imager. Applications for the smart active imager are diverse and include multiple conveyer belt product tracking. Future work relates to designing and demonstrated a fully smart active T/R imager that engages electronically programmable beamforming optics in both the T and R of the smart system for multiple barcode acquisition with automatic feedback control to exploit the full capabilities of the agile pixel (and/or pixel set) concept.

REFERENCES

[1] Golnabi, H. and Asadpour, A., "Design and application of industrial machine vision systems," ELSEVIER Robotics and Computer-Integrated Manufacturing 23(6), 630–637 (2007).

[2] Malamas, E. N., Petrakis, E. G. M., Zervakis, M., Petit, L. and Legat, J. D., "A survey on industrial vision systems, applications and tools," ELSEVIER Image and Vision Computing 21(2), 171–188 (2003).

[3] Betke, M., Gips, J. and Fleming, P., "The Camera Mouse: Visual Tracking of Body Features to Provide Computer Access for People With Severe Disabilities," IEEE Transactions on Neural Systems and Rehabilitation Engineering, 10(1), 1-10 (2002).

[4] Burton, A. M., Wilson, S., Cowan, M. and Bruce, V., "Face Recognition in Poor-Quality Video: Evidence from Security Surveillance", Psychological Science 10(3), 243-248 (1999).

[5] Hellekson, R., Reddersen, B., and Campbell, S., "Optical system design for high speed bar code scanning," Proc. SPIE 0741, Design of Optical Systems Incorporating Low Power Lasers, 94 (1987).

[6] Shellhammer, S. J., Goren, D. P. and Pavlidis, T., "Novel signal-processing techniques in barcode scanning," IEEE Robotics & Automation Magazine 6(1), 57-65 (1999).

[7] Yalcinkayaa, A. D., Ergenemanb, O. and Ureyb, H., "Polymer magnetic scanners for bar code applications," Sensors and Actuators A: Physical 135(1), 236–243 (2007).

[8] Yaqoob, Z., and Riza, N. A., "Passive Optics No-Moving-Parts Barcode Scanners," IEEE Photonics Technology Letters 16(3), 2004.

[9] Riza, N. A., Multiplexed Optical Scanner Technology, US Patent No. 6,687,036, (2004).

[10] Riza, N. A., and Bokhari, A., "Agile optical confocal microscopy instrument architectures for high flexibility imaging," Proc. SPIE 5324, Three-Dimensional and Multidimensional Microscopy: Image Acquisition and Processing XI, 77, (2004)

[11] Riza, N. A., Webb-Wood, G., Kik, P. G., and Sheikh, M., "Demonstration of three-dimensional optical imaging using a confocal microscope based on a liquid-crystal electronic lens," SPIE Optical Engineering 47(6), (2008).

[12] Riza, N. A. and Reza, S. A., "Smart Agile Lens Remote Optical Sensor for Three Dimensional Object Shape Measurements," OSA Applied Optics, 49, 1139–1150 (2010).

[13] Riza, N. A., Reza, S. A. and Marraccini, P. J., "Digital Micro-mirror Device-based broadband optical image sensor for robust imaging applications," Optics Communications 284(1), 103-111, (2011).

[14] Amin, M. J. and Riza, N. A., "Smart Laser Scanning Sampling Head Design for Image Acquisition Applications," OSA Applied Optics 52(20), 4991-4996 (2013).

[15] Hecht, E., Optics, 4th Edition, Pearson, (2002).

[16] Joseph, E., and Pavlidis, T., "Bar code waveform recognition using peak locations," IEEE Transactions on Pattern Analysis and Machine Intelligence 16(6), 630-640 (1994).

[17] Muniz, R., Junco, L. and Otero, A., "A robust software barcode reader using the Hough transform," IEEE International Conference on Information Intelligence and Systems, 313-319 (1999).

[18] Madej, D., "Reversing Convolution Distortion in a Laser Barcode Scanner," IEEE Workshop on Automatic Identification Advanced Technologies, 140-145 (2007).

[19] Bodnar, P. and Nyul, L. G., "Improving Barcode Detection with Combination of Simple Detectors," Eighth International Conference on Signal Image Technology and Internet Based Systems (SITIS), 300-306 (2012).

[20] Riza, N. A. and Reza, S. A., "Noncontact distance sensor using spatial signal processing," OSA Optics Letters 34(4), 434-436 (2009).
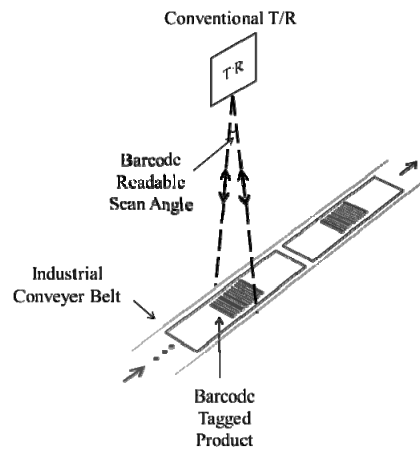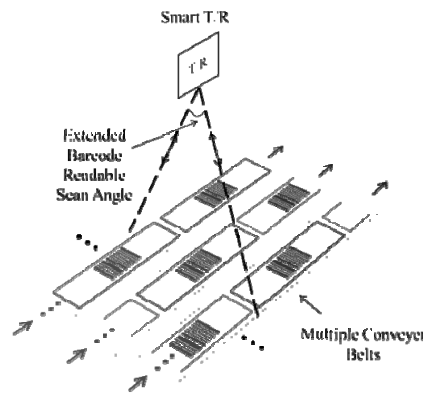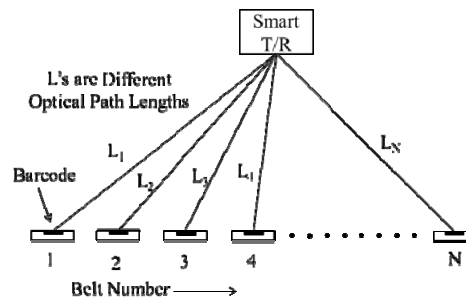
Fig. 1. (a) Barcode reading via conventional limited Depth of Field (DOF) Transmitter/Receiver (T/R) that restricts viewing to a single conveyer belt, (b) Barcode reading via enhanced DOF smart T/R that allows extended viewing of multiple conveyer belts, and (c) Side-view of the system in (b) showing the different optical path lengths from the T/R module to conveyer belt locations.

(a)

(b)
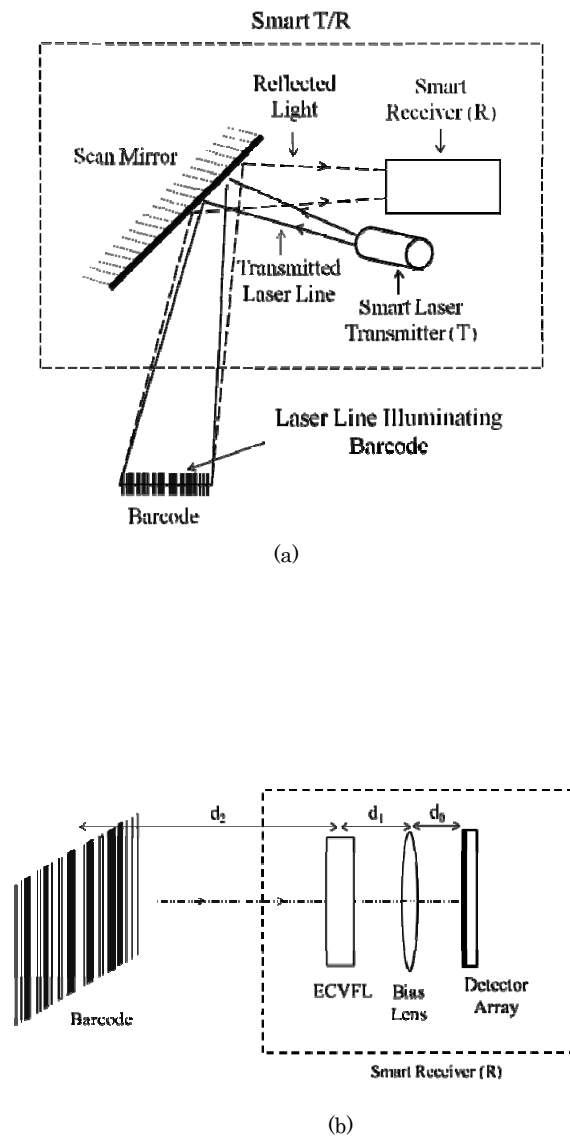
Fig. 2. (a) Proposed smart T/R design using Electronically Controlled Variable Focal-Length Lenses (ECVFLs) in both the T and R units and (b) Proposed smart optical receiver (R) design using an ECVFL-BL lens combination for flexible DOF and increased Field of View (FOV) image capture. These T & R units are special cases of our proposed agile pixel (and/or pixel set) concept in T/R imaging.

(a)

(b)

(c)
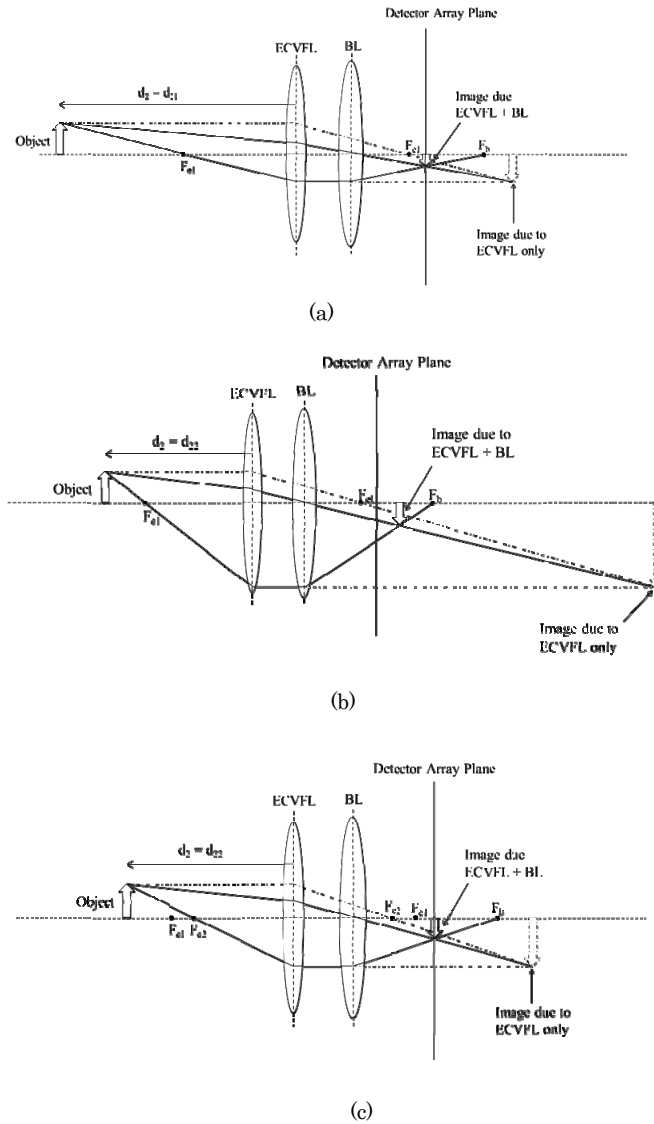
Fig. 3. Ray trace diagrams for the proposed Fig.2 (b) Receiver (R) showing (a) Image of barcode at $d=d_{21}$ falls on CCD Plane with $Fe=F_{e1}$, (b) Image of barcode at $d=d_{22}$ does not fall on CCD Plane with $Fe=F_{e1}$, and (c) Image of barcode at $d=d_{22}$ falls on CCD Plane with $Fe=F_{e2}$
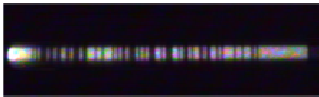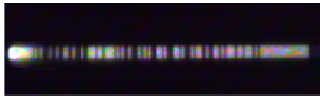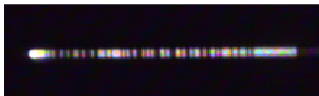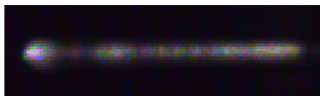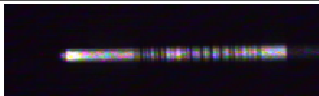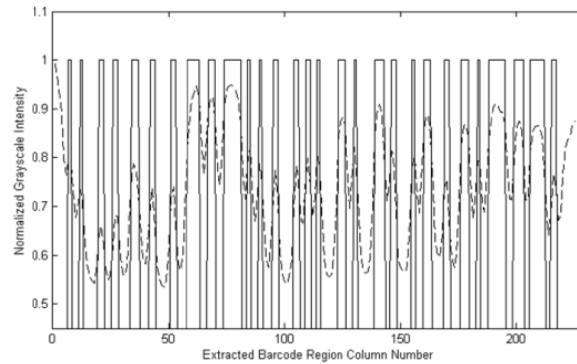
Fig. 4. Comparison of images captured via the smart T/R imager versus a Fixed lens imager.
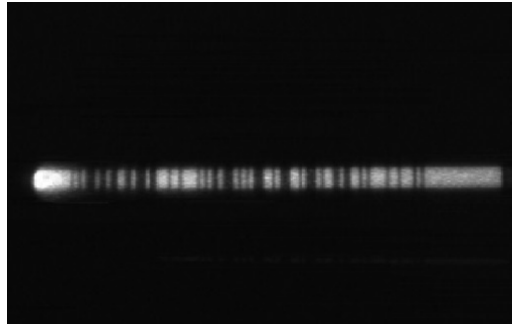
(a)
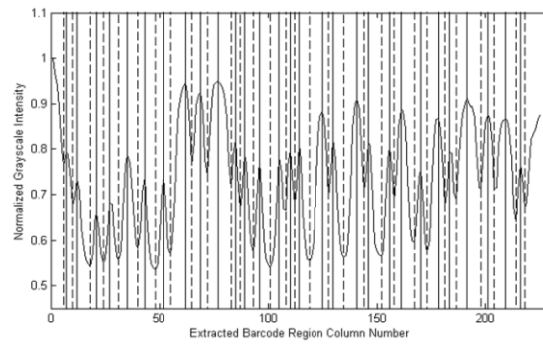
(b)

(c)

Fig. 5. Peak Recognition and thresholding based algorithm results following each step showing (a) Raw image to be fed into the algorithm, (b) Useful region extracted, and Local minima (dashed vertical lines) and local maxima (bold vertical lines) detected, and (c) Step function generated via thresholding between consecutive minima and maxima.

	Smart, $d_2 - 17.5$ cm	Fixed, $d_2 - 17.5$ cm
Original Barcode		
Algorithm Read		
Percentage Barcode Recovered	94.7 %	46.8 %

Fig. 6. Results for the barcode reading software algorithm applied to captured raw images via the smart T/R imager and fixed lens imager for $d_2 = 17.5$ cm.